Journal of Engineering Research and Applied Science
Available at www.journaleras.com
Volume 9 (2), December 2020, pp 1477-1485
ISSN 2147-3471 © 2020

Aerodynamic investigation of vehicle coating materials

K. Ermis[1,a], A. Okan[2]

[1]Sakarya University of Applied Sciences, Department of Mechanical Engineering, Sakarya, Turkey.
[2]Sakarya University of Applied Sciences, Institute of Science, Automotive Eng., Sakarya, Turkey.

Accepted 8 September 2020

Abstract
Aerodynamic drag coefficient, which is one of the most prominent issues when it comes to resistances affecting vehicle movements, has been the agenda of many studies from past to present. Vehicle body coating materials such as paint, paste, etc. used in vehicles can improve the aerodynamic properties of the vehicle and reduce fuel consumption. In this study, the effects of surface roughness differences created by coating materials such as paint, primer paste, special applications, etc. on the aerodynamic friction coefficient were investigated using the finite element method. By using the packaged computer program, the aerodynamic drag forces and aerodynamic drag coefficients encountered at different speeds between 40 km/h - 150 km/h were calculated by defining the body parts and front-rear glass parts separately with the industry-specific roughness values. Appropriate roughness values are calculated and then the results are presented graphically and visually. Three different paint roughness values, which are low (Ra = 0.000000351 m), medium (Ra = 0.000001032 m), and high (Ra = 0.00000148 m), and a commonly used fluoropolymer, also called Teflon (Ra = 0.00000524 m) were used. It has been observed that changes in pavement aerodynamic drag coefficient increase with increasing levels of roughness. According to the low paint roughness value, there was an increase in the aerodynamic resistance coefficient compared to the medium roughness value, an increase of 0.000612529%, an increase in the aerodynamic resistance coefficient compared to the high roughness value, an increase of 0.00104783%, and an increase in the aerodynamic resistance fluoropolymer roughness value was 0.091195826%.

Keywords: aerodynamics, finite element method, friction coefficient, surface roughness, computational fluid dynamics.

1. Introduction

Although aerodynamics is a part of gas dynamics and has similarities, it is differently limited to air. It is a very important discipline for the automotive industry. The power generated in vehicles resists five resistance during vehicle movement. These resistances are rolling resistance, hill resistance, acceleration resistance, powertrain resistance, and aerodynamic resistance. A passenger vehicle with a speed of 100 km/h spends 60% of its power to overcome aerodynamic resistance force (aerodynamic resistance) caused by friction with air, 20% to wheel friction force (rolling resistance), 20% to other forces that prevent movement. Fuel consumption is reduced by improving the aerodynamic properties of the vehicle [1-2]. Coating materials have a certain roughness value. This roughness value creates various negative effects on the aerodynamic drag force acting on the moving vehicles by increasing the friction situation. [2].

Asim et al. (2019) conducted a study using the finite element method on the effect of the surface roughness of truck trailers on the aerodynamic drag coefficient. They found that the aerodynamic drag coefficient increased at high speeds [3]. Mallick et al. (2018) researched the effects of surface roughness on the aerodynamic drag coefficient on cylindrical objects [4]. Sirenko et al. (2012) made improvements to the aerodynamic drag coefficient by changing the shape of the rear body of an off-road vehicle. He stated that an advantage of 26% would occur because of the study [5]. Solmaz (2010) analyzed a bus model with computational fluid dynamics

(HAD) method using a package program and encountered an aerodynamic drag coefficient of 0.65 according to experimental results and 0.66 according to Ansys results [6]. The first wind tunnel was built in 1894 and it was determined the aerodynamic drag coefficient of a vehicle by H.F. Philips [7].

While liquids can move non-moving objects, moving objects can pass through stationary fluids. Although these two situations may seem different from each other, what matters is the relative motion state between each

[a] Corresponding author; ermis@subu.edu.tr

other. These movements are called external flows. The movement of air around a moving vehicle or the movement of wind around a vehicle. External flows are

In this study, based on mathematics and turbulence kinetics energy equations are defined for the numerical study. The method is explained with roughness height, model geometry, Reynolds number depending on velocity, and mesh knowledge for the analysis. Results too complex to be solved by mathematical formulas. For this reason, experimental methods or numerical methods are used to solve these solutions.
of average aerodynamic drag forces acting on the vehicle at different roughness values, and aerodynamic drag forces at different coating materials between 40 km/h-150 km/h. Fluoropolymer is a high value of aerodynamic drag coefficient according to the other coating materials at the designed vehicle.

2. Mathematical approach

The programs used in CFD (Computational Fluid Dynamics) solutions with the developing technology; Together with these experimental methods, they can be indispensable methods for flow analysis. While the pressure resistance is zero on the surfaces parallel to the flow, Surface friction resistance is zero on surfaces positioned perpendicular to the flow. Friction resistance is directly proportional to viscosity. Since the Reynolds number is inversely proportional to the viscosity, the friction resistance can be neglected at high Reynolds numbers [7]. The Reynolds number is known as the number that determines the flow characteristic.

$$Re = \frac{VL}{v} \quad (1)$$

Where Re is Reynolds number, V is the flow rate, L is the length of the surface affected by the fluid and ν is the kinematic viscosity of the fluid.

When the fluid flows over the surface, the surface will resist its motion, which is called drag. Aerodynamic drag is the sum of pressure drag and viscous drag. The pressure drag is the most dominant one of both. The pressure drag is caused due to the shear forces acting between the two layers of fluid.

$$C_d = \frac{F}{0.5\rho V^2 A} \quad (2)$$

Where F is the drag force, Cd is aerodynamic drag, ρ is the air density, A is the effective frontal area, V is the velocity.

The theoretical analysis of turbulent skin friction drag is complex; an exact solution has not been established. The available solutions are generalizations of experimentally determined velocity distributions across the boundary layer.
The friction resistance is directly proportional to the surface area. For this reason, surface friction in commercial vehicles with large front surface area, hence the aerodynamic coefficient of resistance is greater. The contribution of the surface roughness to the aerodynamic drag coefficient in laminar flow is zero. Surface roughness; It is a parameter that affects the aerodynamic coefficient of resistance in turbulent flows [7].

In the K-omega model, k is omega and indicates the energy loss, while the turbulent flow indicates the kinetic energy. The k-omega turbulent flow model was used in this analysis, as it is a more sensitive model than the k-epsilon model in boundary layer conditions where the flow is more intense. Different turbulence models are found in the simulation ranging from steady-state approaches, k-epsilon and k-omega (SST), transient models (DDES), and stress-blended eddy simulation (SBES) [8]. Analyzes made with SST omega and realizable k-epsilon solution models give results with an error of less than 0.5%. In the aerodynamic analysis guide published by SAE (Society of Automotive Engineering), it was seen that the k-omega model gives high accuracy results [9].

In the Ansys analysis, the K-omega model has used an analysis of the vehicle's aerodynamics. The turbulence kinetic energy, k, and the specific dissipation rate, omega, are obtained from the following transport equations:

$$\frac{\partial}{\partial t}(\rho k) + \frac{\partial}{\partial x_i}(\rho k u_i) = \frac{\partial}{\partial x_j}\left(\Gamma_k \frac{\partial k}{\partial x_j}\right) + G_k - Y_k + S_k \quad (3)$$

and

$$\frac{\partial}{\partial t}(\rho w) + \frac{\partial}{\partial x_i}(\rho w u_i) = \frac{\partial}{\partial x_j}\left(\Gamma_w \frac{\partial w}{\partial x_j}\right) + G_w - Y_w + S_w \quad (4)$$

In these equations, Gk represents the generation of turbulence kinetic energy due to mean velocity gradients. GW represents the generation of omega. Γk and Γw represent the effective diffusivity of k and omega, respectively. Yk and Yw represent the dissipation of k and omega due to turbulence. All of the above terms are calculated as described below. Sk and Sw are user-defined source terms.

3. Method

Aerodynamic drag force and aerodynamic drag coefficient calculations are generally made with package programs today. Drawing geometry, drawing the appropriate network structure to be used in the finite element method, entering appropriate input parameters for this structure and starting the solution, velocity vectors, and pressure changes in the model to be values according to the sample model and the solution processes were carried out with Ansys Fluent 19.2 encountered in the solution and these processes are the process stages. All these processes are defined as computational fluid dynamics (CFD).

With this Sun Design Modular program, presentation 1/20 a ready-made vehicle design was prepared; The network structure was realized, the input of learning package program. The access type of vehicle model used in the study is shown in Figure 1

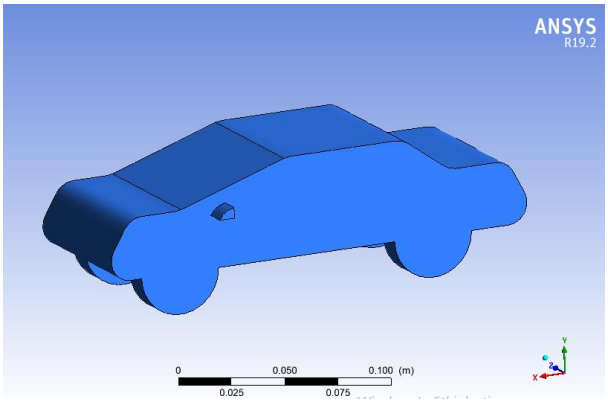

Figure 1. General view of the vehicle to be used in the analysis

The hood of this introduced sample vehicle model; Considering the paint with three different roughness values, fluoropolymer coating, and a completely smooth surface, different measurements were made for five different applications in total. 9.40×10^{-8} m fixed glass average roughness value was used for the front and rear windows of the vehicle [10].

Apart from the mutual values in Table 1, the roughness value of the steel material generally preferred in automotive bodywork varies between 6×10^{-7} m and 8×10^{-7} m [10]. This value can be said that a paint material with low roughness, which will be in the water, has a lower roughness value than an unpainted vehicle body and is beneficial in reducing the aerodynamic drag coefficient. The corresponding roughness is given in table 1.

Table 1: Roughness values used for measurements.

Material	Roughness Height (Ra), m
Paint - 1	3.51×10^{-7}
Paint - 2	1.03×10^{-6}
Paint - 3	1.48×10^{-6}
Fluoropolymer	5.24×10^{-6}
Glass	9.40×10^{-8}

As can be seen from the visuals below of the 1/20 vehicle model to be used in the analysis; Figure 2 is defined as the superstructure and Figure 3 is defined as glass. Vehicle parts of the design published in blue are considered as superstructure as seen in Figure 2.

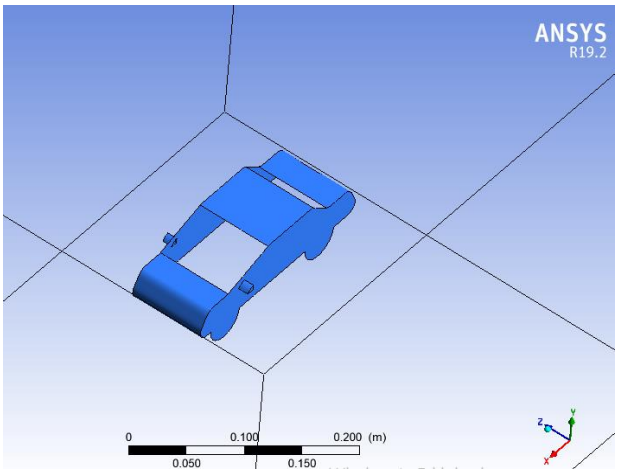

Figure 2. Body view of the vehicle used in the analysis

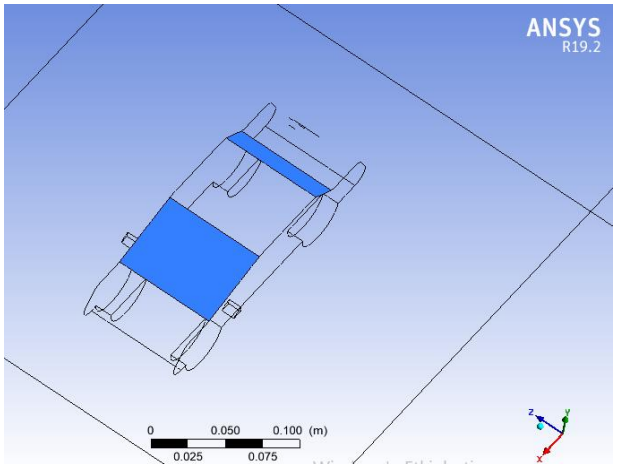

Figure 3. Front and rear window views of the vehicle used in the analysis

By changing, the values are given in Table 2, aerodynamic drag force and coefficient measurements were made between 40 km/h and 150 km/h speed. The front and rear camera sections in Figure 3 can be given in the analysis given above in the graph displayed in Table 1.

The model such as traveling in Figure 1, Figure 2, Figure 3 was created in Ansys Fluent 19.2 package program with 10 km/hour between speeds of 40 km/ and 150 km/ in a wind tunnel. Speed increases and five different roughnesses in speed. The Reynolds Number table calculated by examining this velocity and the design to be examined suggest in Table 2.
Considering that the surface roughness in laminar flow does not affect the aerodynamic coefficient of friction, the analyzes will be made within the framework of the turbulent flow model [7].

The turbulent flow model, in which the distortions in the flow lines are written, can be considered as the most suitable model for this research. The flow length value indicated in Table 2 is the flow length in the wind tunnel of the design. Although the package program to be used for the learning turbulence flow model provides a flow model, the most used models are K-epsilon and K-omega models. These package programs perform computational representation fluid dynamics solutions using continuity and momentum equations in detail below.

The most important parameter for computational fluid dynamics analysis to give accurate results is mesh construction quality. The important point in network structures is not the density of the network structure, but the ratio of the lengths of the network to the neighboring networks. The medium density mesh model is considered sufficient for the subject study [12]. For this study, the number of networks and the number of network nodes that are the junction points of the networks is shown in Table 3.

Table 2. Reynolds Numbers calculated considering the speeds to be examined and the model geometry for 0.23 flow length.

Speed (m / s)	Speed (km / h)	Reynolds Number
11.11	40	1.44×10^5
13.89	50	1.79×10^5
16.67	60	2.15×10^5
19.44	70	2.51×10^5
22.22	80	2.87×10^5
25	90	3.23×10^5
27.78	100	3.59×10^5
30.56	110	3.95×10^5
33.33	120	4.31×10^5
36.11	130	4.67×10^5
38.89	140	5.02×10^5
41.67	150	5.38×10^5

Table 3. Mesh data

	Element Number	Nodes
Mesh Data	107365	93935

4.Reults

Aerodynamic drag forces vary in direct proportion to the square of the speed. While extracting these values, the scale value of 1/20 was taken into account and 400, resulting in the results shown in the graphic, multiplied the front surface area. In the graph shown in Figure 4, aerodynamic resistance forces at a speed of 100 km/hour and the changes of these forces according to the body covering material can be seen.

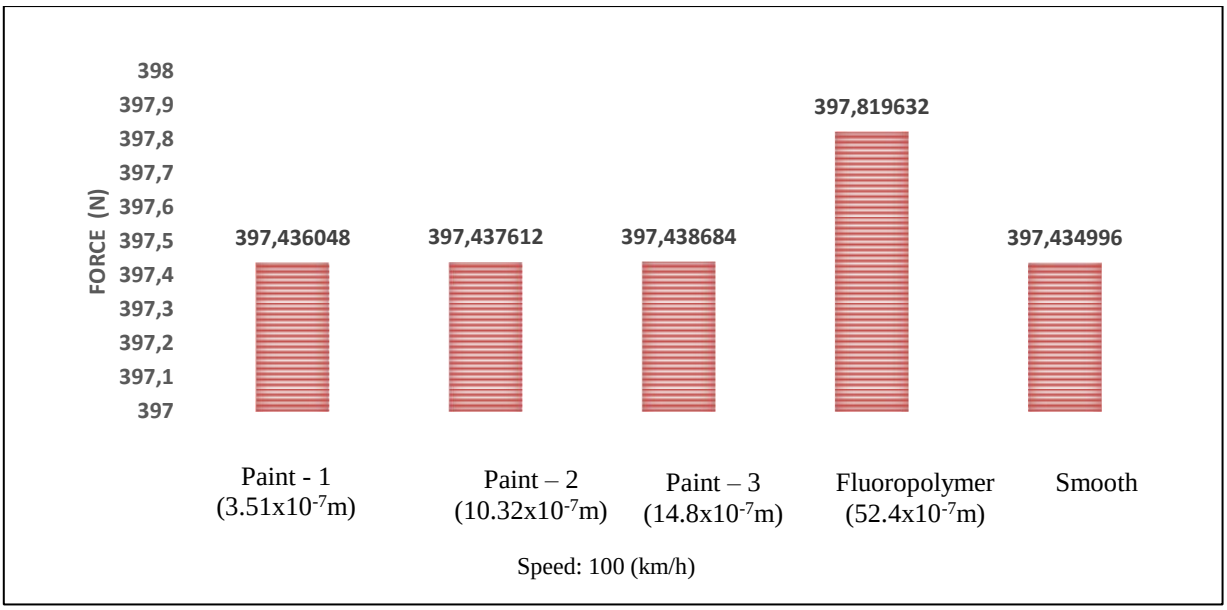

Figure 4. Change of aerodynamic drag forces at 100 km/h

As can be seen from Figure 4, with the high roughness value of fluoropolymer coating vehicles,

the aerodynamic resistance force value encountered is higher. Aerodynamic drag coefficient (FCD) values calculated by the package program in three different paint roughness values converted to real size according to the vehicle scale as shown in Table 4.

Table 4. Aerodynamic drag force values for different coating and smooth surface (no coating)

SPEED (km/h)	AERODYNAMIC DRAG FORCE (N)				
	Low Roughness	Mid Roughness	High Roughness	Fluoropolymer	Smooth Hood
40	65.480912	65.481280	65.481520	65.483676	65.480664
50	101.492056	101.492648	101.493072	101.500180	101.491680
60	145.271872	145.272584	145.273072	145.297312	145.271388
70	196.596104	196.596900	196.597360	196.661432	196.595468
80	255.825716	255.826776	255.827512	255.960668	255.825244
90	322.778776	322.779592	322.780148	323.015088	322.778528
100	397.436048	397.437612	397.438684	397.819632	397.434996
110	479.794320	479.797640	479.799880	480.378360	479.792320
120	569.525760	569.531000	569.534400	570.340040	569.522880
130	667.271960	667.277440	667.282040	668.364280	667.269200
140	772.725280	772.732480	772.737840	774.151520	772.721080
150	885.875600	885.883520	885.889840	887.690560	885.869800

As can be seen in Table 4, aerodynamic resistance forces in three different roughness dye values make changes that affect the second or third steps after the comma on average. However, the variations in aerodynamic resistance forces between the smooth body structure and the fluoropolymer coating with high roughness are seen. Accordingly, for a vehicle traveling at a speed of 100 km / h, it is seen that an aerodynamic resistance force difference of 0.97% occurs. Figure 5 shows the column graph of the average aerodynamic resistance forces acting on the vehicle at different roughness values between 40 km/hour -150 km/hour. Accordingly, the highest aerodynamic drag effect was realized in the fluoropolymer coating is expected. It is seen that there is not much difference in strength in vehicles designed with smooth coating and low roughness paint. The aerodynamic resistance coefficient graph that emerged as a result of the forces acting on the vehicle in the range of 40 km/hour - 150 km/hour is shown in Figure 6.

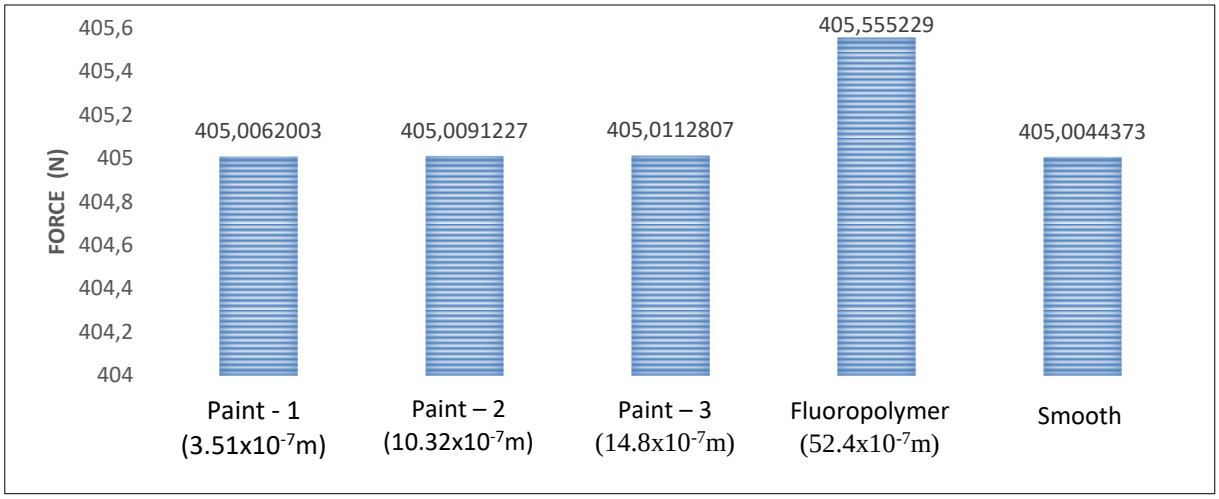

Figure 5. Average aerodynamic drag forces (N) acting on the vehicle at different roughness values between 40 km/h - 150 km/h.

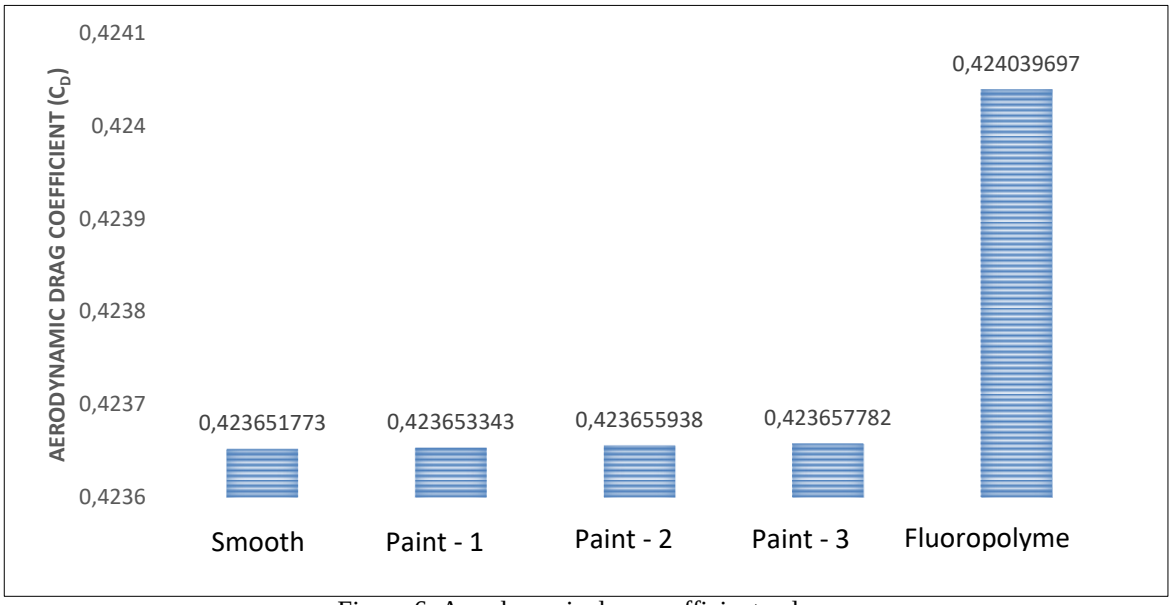

Figure 6. Aerodynamic drag coefficient values

The velocity images of the design were also created along with the aerodynamic drag force and aerodynamic drag coefficient calculations. Accordingly, as seen in Figure 7, the velocity distribution around the design is given.

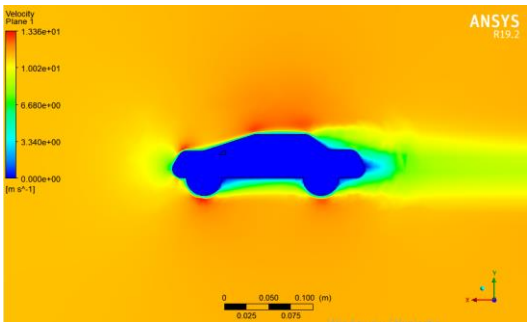

Figure 7. Body with low paint roughness at 40 km/h.

As can be seen, it is seen that the speed of the vehicle is up to 45 km/h, although the entry speed is 40 km/h under normal conditions in the separation area above and below the front bumper and the rear trunk.
In Figure 8, it is seen that speeds reach up to 160 - 170 km/h in the wind tunnel with a vehicle speed of 150 km / h in the separation area above and under the front hood and on the rear trunk. The same conditions are also valid for the fluoropolymer coating, which is accepted as the maximum roughness in our study.

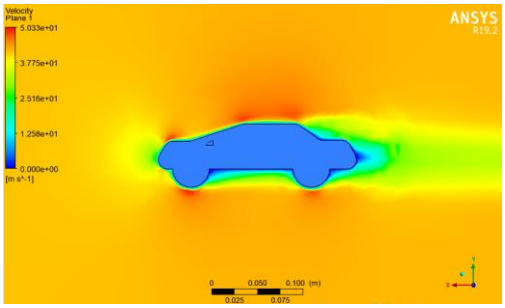

Figure 8. Body with low paint roughness at 150 km/h

The same conditions are also valid for the fluoropolymer coating, which is accepted as the

maximum roughness in our study. The speed images of the fluoropolymer coating at speeds of 40 km h and 150 km h are shown in Figure 9 and Figure 10.

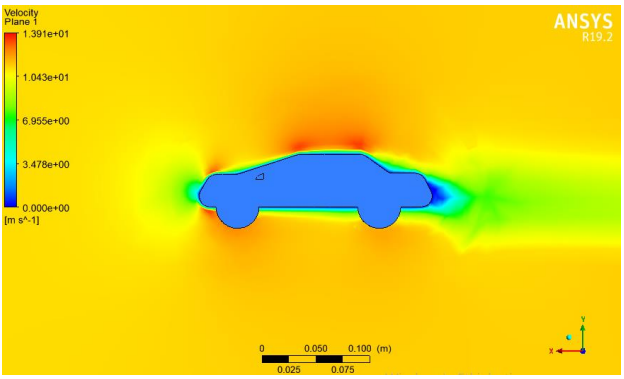

Figure 9. The location around a vehicle with a fluoropolymer bodywork at 40 km/h.

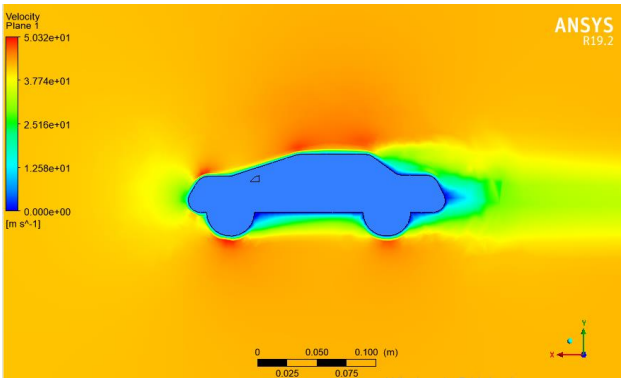

Figure 10. The location around a vehicle with a fluoropolymer bodywork at 150 km/h.

5. Conclusions and discussion

These roughness values, which are different by 1/1000000 of the meter (m), affected the aerodynamic drag force and aerodynamic drag coefficient values as can be predicted. In these analyzes performed on three different paint roughness (low, medium, high), fluoropolymer coating and flathead, force changes occurring in the second or third stage after the decimal point as a result of calculations made over aerodynamic resistance force; Maximum roughness makes an average of 0.205% difference between fluoropolymer coating and zero roughness smooth coating.

Although there are differences between the high roughness paint and low roughness paint coating in the fourth or fifth stages after the comma in terms of aerodynamic resistance coefficients, the difference in the zero roughness value with the fluoropolymer coating starts to occur in the third step comma. Accordingly, according to the low paint roughness value, 0.000612529% increase in aerodynamic resistance coefficient compared to medium roughness value, 0.00104783% increase in aerodynamic resistance coefficient compared to high roughness value and 0.091195826% increase in aerodynamic resistance coefficient according to fluoropolymer roughness value.

References

[1] Çakmak, M.A, Investigation of vehicles as aerodynamically, Mühendis Makina, 41, 2000, 489.

[2] Bayındırlı C., Akansu Y.E., Salman M.S. The determination of aerodynamic drag coefficient of truck and trailer model by wind tunnel tests, International Journal of Automotive Engineering and Technologies, 5(2), 2016, 53-

60.
[3] Asım T., Ubbi, K., Mishra, R. and Nsom, B. Effect of surface roughness on the aerodynamic performance of an articulated truck-trailer assembly, The 24th Congrès Français de Mécanique (CFM 2019), Brest, France, 2019.
[4] Mallick K. Wandera L., Bhattarai N., Hostache R., Kleniewska M., Chormanski J. A critical evaluation on the role of aerodynamic and canopy–surface conductance parameterization in seb and svat models for simulating evapotranspiration: a case study in the upper biebrza national park wetland in Poland, Water, 110(12), 2018, 1-27.
[5] Sirenko V., Pavlovs'ky R., Rohatgi U.S. Methods of reducing vehicle aerodynamic drag, ASME 2012 Fluids Engineering Division Summer, 2012, 97-102.
[6] Solmaz, H. Determination of wind resistance coefficients of different vehicle models in a wind tunnel, Master Thesis, Gazi University Science Institute, Ankara, 2010, 43-47.
[7] Cengel Y, Cimbala J. Fluid Mechanics Fundamentals and Applications, 3rd Edition, The McGraw Hill, NY, USA, 2014.
[8] Buscariolo F.F., Magazoni F, Wolf M., Maruyama F.K., Alves J.C.L., Volpe L.J.D. Analysis of turbulence models applied to CFD drag simulations of a small hatchback vehicle, S SAE Technical Paper 2016-36-0201, 2016.
[9] SAE Standards, Guidelines for Aerodynamic Assessment of Medium and Heavy Commercial Ground Vehicles Using Computational Fluid Dynamics, J2966-201704, 2017.
[10] Vazirian M.M, Charpentier, T.V.J., Penna M.O., Neville A. Surface inorganic scale formation in oil and gas industry: as adhesion and deposition processes, Journal of Petroleum Science and Engineering, 137, 2015, 22-32.
[11] Streitberger HJ., Dossel KF. Automotive Paints and Coatings, Wiley-VCH Verlag GmbH & Co. KGaA: Weinheim, Germany, 2008.
[12] Unaune, S.V., Sovani, S.D., Kim, S.E. Aerodynamics of a Generic Ground Transportation System: Detached Eddy Simulation, SAE International, 2005, 45-60.